Nigerian Journal Of Materials Science and Engineering

(NJMSE)

Volume 10 Issue 1 ISSN 214-453-2 May 2020

Materials Science & Technology Society of Nigeria (MSN)

NIGERIAN JOURNAL OF MATERIALS SCIENCE AND ENGINEERING
NJMSE
ISSN 214-453-2

An International Journal of the Materials Science and Technology Society of Nigeria

Nigerian Journal of Materials Science and Engineering
Volume 10 Issue 1 May 2020

Nigerian Journal of

Materials Science and Engineering (NJMSE)

Materials Science & Technology Society of Nigeria (MSN)

Volume 10 Issue 1, May 2020
ISSN 214-453-2

Published by

Materials Science and Technology Society of Nigeria (MSN)
National Headquarters
Engineering Materials Development Institute (EMDI)
Km. 4 Ondo Road,
P. M. B. 611, Akure. Nigeria
Tel.: +234-803-471-8487; +234-803-703-3052; +234-806-220-7420

http://njmse.msn.ng
NJMSE@msn.ng; njmse.msn@gmail.com; editorinchief@msn.ng; njmsemanagingeditor@msn.ng;
bbabatop@oauife.edu.ng;giwafat2002@yahoo.com

(NJMSE - An International Journal of the Materials Science and Technology Society of Nigeria)

Editorial Comment

It is a great pressure for the editorial board of the Nigerian Journal of Materials Science and Engineering (NJMSE) to present Volume 10 Number 1 of the journal for 2020 for the world research and development community.

The Materials Science and Technology Society of Nigeria (MSN), as a professional learned body, has made the publication of this research journal to be of very good quality and high standard comparable to any in her class. Our major thrust is to disseminate materials science and engineering and allied research activities from Nigeria, Africa and the world over. We are slowly and gradually impacting on the research community work with this specialised journal from a reputable learned and professional body in Nigeria. We are presently not insisting on number but we very much believe, with the thoroughness of our approach to the review and assessment process, we are convinced that with our resolve to publish quarterly, the board is convinced that more researcher would take advantage of this.

As a journal whose policy is to maintain the standard best practices and in addition to help young researchers to advance in the art and science of scientific findings dissemination, had faced tremendous challenges which were expected. It is heart-warming that we can look back and be glad to see the society publishing the 10th volume. These volumes and the previous ones would be available for FREE downloading on our society website (www.msn.ng) through a link prior to the specialised journal website to be available soon. Arrangements are in advanced stages for the hosting of this journal by reputable international online submission system are being worked on.

Volume 10 (2020) Number 1 consists of eight (8) high standard articles covering different specialised areas of materials research. It is our hope that this humble effort, presently by voluntary efforts of senior members of the Society, at disseminating research findings as put together in this volume which have contributed to the body of knowledge, would have enriched the information base and complemented Materials Research efforts from around the world.

We appreciate all our reviewers and associate editors involved for their prompt action on the manuscripts and cooperation as we look forward to submission of manuscripts which can be forwarded as detailed below.

Babaniyi Babatope. (PhD,MBA,FMSN,FIMMM(UK))
Editor-in-Chief.
Department of Physics and Engineering Physics,
Advanced Nanostructured Materials and Devices Research Group
Obafemi Awolowo University, Ile-Ife. Nigeria.
bbabatop@oauife.edu.ng
editorinchief@msn.ng; njmse.editor.in.chief@gmail.com.

Manuscripts can also be submitted and copied to:

Managing Editors, NJMSE.
njmsemanagingeditor@msn.ng; njmse.msn@gmail.com; njmse@msn.ng.

Editor-in-Chief
editorinchief@msn.ng;njmse.editor.in.chief@gmail.com

Website:
http://njmse.msn.ng/

GUIDE TO AUTHORS

AIM: *T*o improve the international exchange of scientific research in materials science and engineering.

INTRODUCTION

The Nigerian Journal of Materials Science and Engineering (NJMSE) publishes reviews, full-length papers, and short communications recording original research results on, or techniques for studying the relationship between structure, properties, and uses of materials. The subjects are seen from international and interdisciplinary perspectives covering areas including metals, ceramics, glasses, polymers, composite materials, fibers, electronic materials, alternative energy materials, nanostructured materials, nanocomposites, biological, biomedical materials, etc. The NJMSE is now firmly established as the leading source of primary communication for scientists investigating the structure and properties of all engineering materials in Nigeria, Africa and the Rest of the World.

UNIQUENESS OF THE JOURNAL

NJMSE is introduced to publish research findings on current topical issues of interest to both public and private sectors. The scope of the Journal focuses on experimental, empirical and theoretical research in Materials Science and Engineering. Findings from multidisciplinary research covering diverse areas of interest with potential impact on the public and private sectors of both the national and international communities will be priorities of the journal. Our major focus is the use of Materials Science and Engineering principles to solve basic problems peculiar to Africa and the developing world while contributing to knowledge on the global scale.

GUIDE FOR AUTHORS

NJMSE welcomes research papers covering original work that has good potential for practical application. Submission of a manuscript will be held to imply that the work being reported is original and that the result has not been published previously nor been under considerations for publication elsewhere.

MANUSCRIPT PREPARATION

The format of the typescript should be as follows:

The official language of the journal is English. When writing do not mix languages, use US English completely or use UK English completely. It is expected that before submission, the manuscript will have been thoroughly reviewed and written in simple clear expression. Manuscript should be typewritten with double-spacing and 2.54 cm or 1 inch margins on all sides. Manuscripts should be submitted in electronic form and e-mailed directly to the addresses below in MS-Word format, double spacing with graphics at the end. Manuscripts should be arranged in the following order: title page, abstract, introduction, materials and methods, results and discussion, conclusions, acknowledgements, references. The manuscripts should follow the format listed below.

Title: The title page should contain the title [concise but clear expression, written in bold, upper case], followed by the authors [surname first, block letters throughout], and followed by their institutional affiliations and the e-mail address of the corresponding author. In case of many authors, please use numbers to differential their affiliation.

Abstract: An abstract of not more than 350 words should be supplied immediately before the beginning of the paper (Graphical abstracts are also acceptable).

Introduction: This should contain a brief review of literature, clearly stated objectives and justification for the study.

Materials and Methods: This should contain materials preparation procedure and major measurement patterns. Sufficient information should be provided to perform repetition of the experimental work.

Results and Discussion: The result section should contain appropriate tables, figures/illustrations**.** These should be pertinent to the work and should clearly indicate the degree of reliability of results. Tables should be numbered consecutively, with a short descriptive title in upper case (block letters) on top of the table. They should contain no vertical lines and no lines to separate the rows except the heading and the end of the table. Figures, micrographs, or illustrations must be clearly captioned, the captions at the bottom of each figure. Figures may not be used to repeat the information already presented in tables or text or vice versa. Micrographs and illustrations are considered as figures and must be labeled as such.

Conclusions: These should summarize any important conclusions emerging from the work.

Acknowledgements: These should be presented at the end of text and before the references. Technical assistance and advice may be acknowledged. Acknowledgments of financial support can also be stated in this section.

References:

Citing: Reference in the text should be made by the author's last name and year of publication, e.g. (Abel, 2007); (Abel and Babcock, 2007); (Bowen *et al*., 2007). Two papers by the same author in the same year should be distinguished by a suffix, (a, b, etc) e.g. (Madonna, 2006a); (Madonna, 2006b).

Listing: This should be in alphabetical order and should follow this format: Name(s) and initial(s) of author(s), (year of publication), exact title of paper (in quote), the title of periodical, Vol. (number)**:** initial and final page numbers. Please note that only name cited in the text can be used.

Serial: Briant C. L. and Banerji S. K. (1981). Tempered Martensite Embrittlement and Intergranular Fracture in an Ultrahigh Strength Sulfur Doped Steel, *Metall. Trans. A,* 12A:309-319. (Please pay attention to punctuations).

Book: Samuels, L.E. (1982). *Metallographic Polishing by Mechanical Methods,* 3ed., American Society for Metals, Metals, Park, Ohio.

Proceeding: Olorunnisola A. O. (2006). The potentials of bamboo as novel building and furniture production materials in Nigeria, pp.180-185. In *Proc. Nigerian Materials Congress (NIMACON 2006),* (B. Babatope and W.O. Siyanbola, Eds.), organized by Materials Society of Nigeria, 15-18 November 2006, Abuja, Nigeria.

Heading and sub-heading: All headings and sub-headings should be numbered and started from the left hand margin. All headings should be in upper case while sub-headings should be in lower case except the first letter.

Equations: Equations should be distinctly typed using Microsoft equation. Avoid powers of "e" and use "exp". Equations should be numbered consecutively by Arabic numerals in parenthesis at the right margin. In the text, such equation should be cited as Equation (1) etc.

Units and symbols: Symbols, units and nomenclature should conform to the recommendations of the International Union of Pure Applied Chemistry (IUPAC). SI units should be used for physical quantities.

Peer-Review: All submitted manuscripts are subjected to a peer- review process and galley proofs will be sent to the first or corresponding author where necessary.

SUBMISSION OF MANUSCRIPTS

A Processing Fee of N10,000.00 only is payable per article. All submitted articles MUST be accompanied with scanned Bank (detail below) Tellers or On-line transfer receipt as evidence of payment. Send your article(s) and Bank Teller to: njmse@msn.ng; NJMSE.msn@gmail.com. All submission of manuscripts must be sent on-line to fast-track processing and simplify the refereeing process.

PAGE CHARGE

Corresponding Authors of accepted articles will be required to pay a sum of N10,000.00 only as processing fee (at the point of acknowledging receipt of manuscript) and N10,000.00 (non-members and non-financial members of MSN), N5,000.00 (financial members of MSN) after acceptance (or $100.00 USD for processing and acceptance for other countries). They will receive free ecopy of the NJMSE volume in .pdf version. The ecopy is available online at http://njmse.msn.ng and can be downloaded free. However, printed copy(ies) may be requested for extra payment.

COPY RIGHT

Submission of an article for publication implies the transfer of the copyright of the manuscript from the author(s) to the publisher upon acceptance and that the manuscript has not been previously published elsewhere. This is the responsibility of the authors. Accepted papers become the permanent property of the publisher and may not be reproduced by any means without the written consent of the Editor-in-Chief.

Account Details: GTB PLC A/C No. 0171794514. Materials Science and Technology Society of Nigeria.

All Correspondence to:

Prof. A. Giwa
NJMSE Managing Editor
Department of Polymer and Textile Engineering
Ahmadu Bello University
Zaria. Nigeria. +2348037033052; +2348025672474
giwafat2002@yahoo.com.

Engr. Adetunji Ogunkoya
NJMSE Desk /Processing Officer,
Engineering Materials Development Institute (EMDI)
Ondo Road, PMB 611,
Akure Nigeria. +2348062207420;+2347081019516

http://njmse.msn.ng/
Emails: njmse@msn.ng; njmse.msn@gmail.com; njmsemanagingeditor@msn.ng;
editorinchief@msn.ng; njmse.editor.in.Chief@gmail.com;

TABLE OF CONTENT

Page No

MICROSTRUCTURE AND HARDNESS PROFILES OF HYBRID LASER-ARC WELDED JOINT FOR ULTRAHIGH-STRENGTH STEEL

Olugbade Emmanuel; **Zhou** Bin; **Ikeagwuonu** Clement; **Yang** Li; **Huang** Gen-Zhe*
School of Mechanical and Electrical Engineering,
Changchun University of Science and Technology, Changchun, Jilin, China.

*** Corresponding author:** Huang Gen-Zhe, Email: huanggenzhe@cust.edu.cn

Abstract
In this investigation, hybrid laser-arc welding was performed on 6-mm thick ultrahigh-strength quenched and tempered steel plates. Laser-arc welds were characterized for hardness and metallurgical properties in three defined cooling cycles. Destructive tests of the joints revealed that the joints were characterized by tensile strength similar to that of the base material. Microstructural characterization was made by optical microscopy, scanning electron microscopy and X-ray diffraction. It was revealed that the weld beads consist of lath martensitic structure with small percentage of retained austenite. Quantitative analysis of mixed microstructures of the heat affected zone (HAZ) revealed 0%, 38% and 62% of the upper bainite for the cooling cycles- cycles A, B and C respectively. In addition, the hardness profile of the cross-section of the weld was characterized by Vicker's microhardness test. The hardness fluctuation values within the HAZ for the cycles A, B and C are 450-510, 370-425 and 320-375 HV respectively, thus increasing as the upper bainite percentage increases with each cycle.

Keywords: Ultrahigh-strength steel, Martensite, Hybrid Laser-Arc Welding, Cooling Curve, HAZ, Hardness.

INTRODUCTION

Ultrahigh-strength steels (UHSSs) are prominent for possessing considerable level of desired mechanical properties such as tensile strength, toughness, impact resistance and low density, resulting in material optimization, affordability and energy conservation (Seede *et al.*, 2020). Being fine tempered and martensitic in microstructure, the UHSSs mechanical properties can be significantly altered when subjected to elevated temperatures during fusion welding processes (Barényi *et. al.*, 2013). The conventional welding operations like the submerged arc welding and the gas-metal arc welding of UHSS material, by reason of the multi-pass requirements of the processes alone, would expose it to elevated temperatures, thereby creating a widespread heat-affected zone (HAZ) in the base material. As a result of this, there is significant retaining of residual stress and uneven cooling of the system (Něměček *et al.*, 2012). This could lead to distortions and structural failure of the material. Hence, the hybrid laser-arc welding (HLAW) remains a welding process suitable for ultra-high strength steel; since HLAW has the advantage of high penetration and deep weld with minimal heat input (Steen, 2004); thus having less thermal effects on the heat affected zones (HAZ) of the material.

Effects of welding parameters on hybrid laser-arc welded high-strength steel plates have been investigated (Mazar *et. al.*, 2018; Ming *et al.*, 2007; Bunaziv *et al.*, 2019). Further reports on the microstructures and mechanical properties of the welded joints reveal how cooling behavior affects the resulting mechanical performance of the weld (Kong and Kovacevic, 2010; Chen *et al.*, 2020; Cao *et al.*, 2011). The cooling manner of a welded joint, being graphically represented by its cooling curve, is a major phenomenon that influences grain morphology and microstructure evolution at that joint (Ma *et al.*, 2014; Kim *et al.*, 2011) . Several researchers have investigated welding properties of high-strength steels, however, not much works have been reported on UHSSs. The purpose of this study is to investigate the microstructures and hardness profiles obtained for three thermal cycles at a certain UHSS material under constant welding parameters.

The basic characteristics of a 6-mm thick hybrid welded joint were obtained by using an optical microscope and a scanning electron microscope (SEM), the weld morphology was analyzed and the detailed features of the microstructures explained. Finally, the hardness profile of the joint was determined by micro-hardness testing process.

MATERIALS AND METHODS

Experimental Equipment

Hybrid laser-arc welding (HLAW) on ultrahigh-strength steel was performed using laser-arc equipment with welding parameters, including welding speed, current/arc voltage, shield-gas flow-rate and laser power listed in Table 1. The welding parameters were arrived at after doing extensive bead on plate welding trials to achieve fully penetrated weld with no undercuts (Frostevarg and Kaplan, 2014; Mazar *et al.*, 2018). Argon gas supplied shielding and plasma purging at the rate of 18 liters per minute (lpm) in the trailing mode with the shielding nozzle inclined at an angle of 30º to the workpiece surface. The laser beam was defocussed by 2 mm while performing the welding experiments. The schematic of the HLAW system and geometry of the plates are shown in Figure 1.

Welding Materials

Welding samples with overall dimensions of 400 mm x 150 mm and 6 mm thickness TS1500 (UHSS) plates were prepared for hybrid laser-arc welding (HLAW) experiments. The as-received steel was manufactured from sequential operations of continuous casting, hot rolling and quenching, followed by a tempering process at 200℃ for 5hr. Table 2 shows the chemical composition of the steel and the nominal composition of filler metal used in the butt HLAW process, coupled with the mechanical properties listed in Table 3. The filler metal of diameter 1.2 mm was a cast, hot-rolled wire, which had been cold-drawn in order to increase its strength and stiffness. Prior to welding, the edges of interest were milled and surface-ground to achieve near flawless Y-groove edge with root face height of 2.5 mm and angle of 30°. A gap of 1 mm was maintained between the plates during welding.

Table 1: Hybrid Laser-Arc Welding Parameters

Welding Current *I (A)*	**Arc Voltage, *U(Volts)***	**Laser Welding speed, *v(m/min)***	**Power, *P(W)***	**Defocus under the Surface of the plate, *f(mm)***	**Laser-Arc distance, d_{LA}*(mm)***	**Shield Gas Type**	**Flow rate *(litre/min)***
220	28.2	0.8	3300	-2.0	3.0	95%Ar+5%CO_2	18

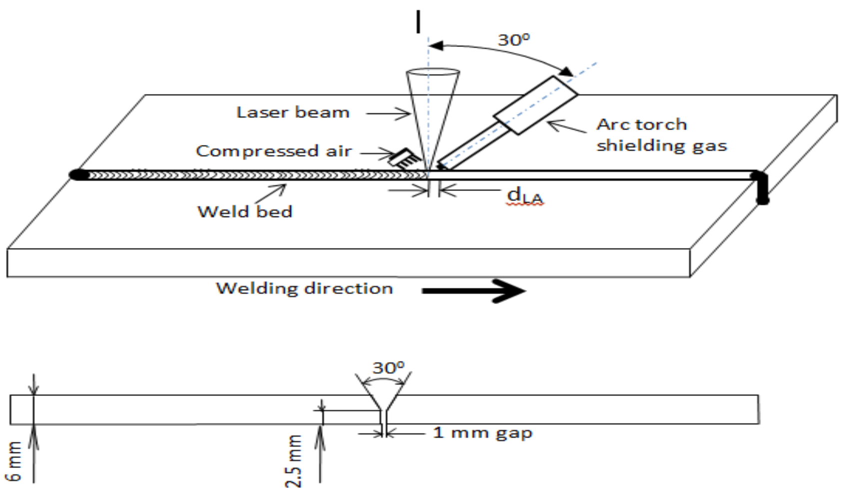

Figure 1: The Schematic Diagram of the HLAW System and Geometry of the Plates

Table 2: Chemical Composition of Ultra-High Strength Steel and Filler Wire (Weight in %)

Material	**Composition**								
	C	**Si**	**Mn**	**S**	**P**	**Cr**	**Mo**	**Ni**	**Fe**
UHSS	0.31	0.34	0.85	0.002	0.011	0.94	-	1.21	Bal
Filler wire	0.02	0.30	6.5	0.01	0.01	19.70	1	10	Bal

Table 3: Mechanical Properties of Ultra-High Strength Steel and Filler Wire

Material	**Mechanical Properties**		
	Yield Strength (MPa)	**Ultimate tensile strength (MPa)**	**Elongation**
UHSS	1300	1500	10%
Filler wire	500	800	-

Thermal Cycle

In order to get different thermal cycles, an automatic heating torch was used to change the thermal Cycle After the welding process. Figure 2 shows the schematic diagram of the locations of a thermocouple in the plate. As it was difficult to monitor the thermal cycle which had almost same heating speed, highest peak temperature and cooling speed, since every point in the plate has its own thermal cycle, three 2-mm diameter holes with different depth were drilled into the plate at the HAZ in order to select one which has nearly the same thermal cycle. The thermocouple used was capable of capturing temperature points at rate 600 points/min; fast enough to follow accurately the high-speed change of the thermal cycle.

The location of the tip of the thermocouple is shown by the macrograph in Figure 3. In this case, it can be observed that, the exact location of tip of the thermocouple is 5.28 mm from the center line, and 3.50 mm from the top surface of the plate.

Inspection Method

Visual and optical inspections were carried out on the weldments to achieve joints devoid of any major defects. Characterization of weld microstructures was achieved by the use of optical microscopy (OP) and scanning electron microscopy (SEM). Microhardness of the welds was measured using Vicker's microhardness tester.

RESULTS AND DISCUSSION

The different thermal cycles at the specified locations is shown in Figure 4; the black line represents the normal thermal cycle, the red line is that of 400 sec-soaking at 400 - 500°C while the blue line is that of 900 sec-soaking at 400-500°C. It was to be observed that these three thermal cycles have almost same heating rate, peak temperatures and cooling rate before soaking at 400 - 500°C. These three thermal cycles are herein referred to as Cycle A, Cycle B and Cycle C respectively.

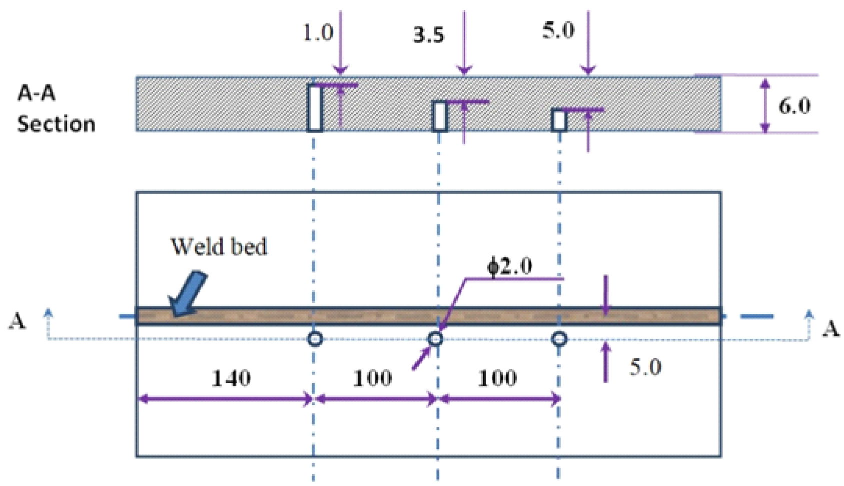

Figure 2: Schematic Sketch of Locations of Thermocouple in the Plate (Dimension in mm)

Microstructural Changes within the Weld Bead

The microstructures of the weld beads after the different thermal cycles are shown in Figure 5 (a, b and c) and are found to comprise of lath martensitic structure. In addition, some laths get through the small angle boundaries between the pre-austenitic dendrites, which reportedly are said to be composed of arrays of edge dislocations (Liu *et al.*, 2017). Through the high-resolution SEM micrograph (Figure 5(d)), it is also proven that the microstructures of weld bead are completely covered by the clusters formed with the parallel laths of the martensitic structure. It can be upheld that there are a lot of alloy elements within the filler wire (6.5Mn-19.70Cr-10Ni) used in this test. Although the chemical compositions of the bead must be diluted by the parent metal, much of the Cr, Mn and Ni must have remained within the bead. As a result, despite being held at 400 - 500°C for 900 sec (Figure 5(c)), it still did not transform to the middle temperature microstructures like troostite or bainitic structures instead, it changes to lath type martensite.

It can therefore be confirmed that the main structures of the beads are composed of the martensitic phase and a little retained austenitic structure. In addition, the thermal Cycle C with the 900 sec soaking at 400 - 500°C contained the higher remained austenite compared to the other two cycles. It is thus predictable that the hardness at the Cycle C must be lower than that of the other two cycles.

Microstructural Changes within the HAZ

It can be easily observed that the area of the HAZ is composed of two different microstructures, the light gray region (A in Figure 6(a)) and the black feather-like regions (B in Figure 6(a)). From the high-resolution SEM microstructures, it is clearly seen that the light gray area consists of lath martensitic phase (Figure 6(b)) and the feather-like region,

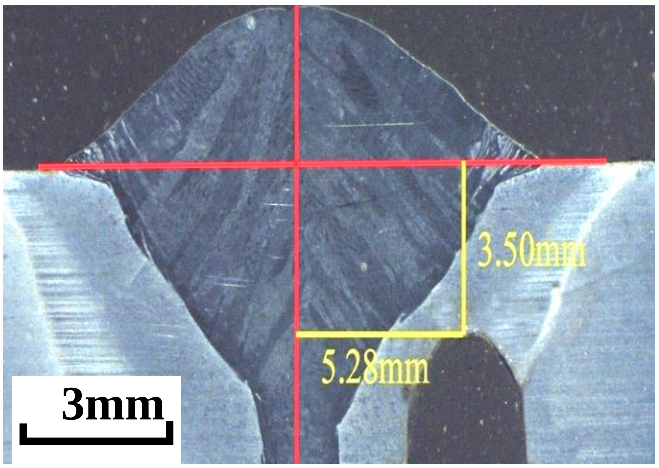

Figure 3: Macrograph of the Location of the Tip of the Thermocouple

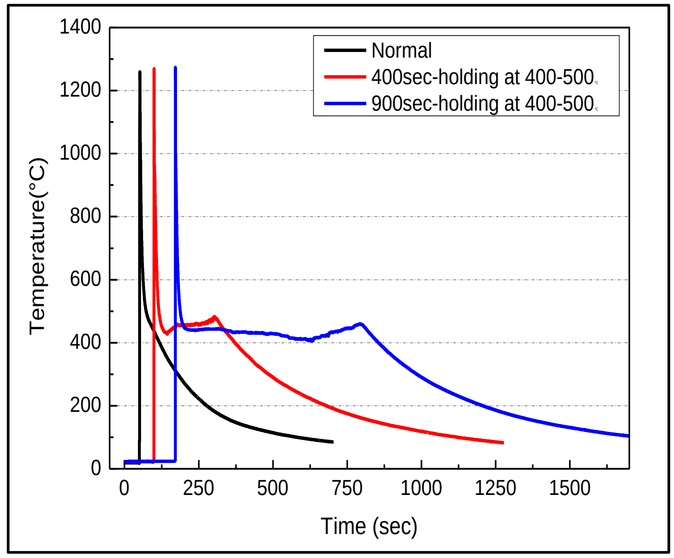

Figure 4: Thermal Cycles A, B And C

the upper bainitic structure (Figure 6(c)), indicates presence of pre-austenite to be transformed to the upper bainite while it is held at 400 - 500℃ for 400 sec.

The transformation of the pre-austenitic phase to the upper bainitic microstructure in the tough high strength steel (ultimate strength-1500 MPa) was caused by the contents of the carbon and alloy elements which are relatively low (0.31C-0.85Mn-0.94Cr-1.21Ni). So, the incubation time for the Continuous Cooling Transformation (CCC-curve) was short. In other word, the C-curve of bainitic transformation must be near the vertical coordinate. As a result, while it was held at 400 - 500℃ for 400 sec, a part of pre-austenitic phase was transformed to the upper bainite (feather like) and some unchanged pre-austenite was transformed to the lath-type martensite afterward (light gray area).

At the normal cooling process (Cycle A in Figure 7(a)), the microstructure of the HAZ was composed of one hundred percent lath-type martensite, whereas the microstructures of the HAZ for the Cycle B and Cycle C consist of mixed upper bainite and lath-type martensite, but the relative amount of the two microstructure was different. That is to say, there was about 38 percent of bainite for the Cycle B while Cycle C (blue column in Figure 7(d)) has 62 percent of it.

Figure 8 demonstrates the optical microstructures of different locations in the HAZ for the. Coarse lath-type martensite can be observed at the regions closer to the fusion line (Figure 8(a) and 8(b)), also there is relatively fine lath-type martensite formed in the middle of the HAZ (Figure 8(c)). Moving farther away from the fusion line, there exists mixed microstructural zone which consists of small grain-like pre-ferrite (white), newly formed fresh martensite (light gray area) and the over-tempered original martensite zone (black zone) as seen in Figure 8(d). This mixed microstructural zone was exactly identical to the two-phase regions of austenite and ferrite in $Fe-Fe_3C$ phase diagram and over tempered region called "soft region". Finally, the farther region (Figure 8(e)) was the parent metal which is not related to the hybrid laser-arc welding process. It is composed of the tempered lath-type martensite as the manufacturing process of plates were sequentially continuous-cast, hot-rolled and finally quenched on line followed by low temperature tempering process at 200℃ for 5 hr.

Hardness Profiles across the Horizontal

The hardness profiles of the whole welded joint for each of the three cycles A, B and C are shown in Figure 9. It was clearly observed that the hardness of the bead for Cycle A was sustained at 460 – 490 HV, whereas the hardness values of the beads for the cycles B and C are almost remained at 400 – 430 HV. This implies that, the parameters of the welding process were the same and microstructures of the three cycles were all lath-type martensite. The hardness values for the normal cooling process (Cycle A) were higher than that of the 400 sec-soaking (Cycle B) and 900 sec-soaking (Cycle C) at 400 - 500℃ and about 60 HV.

We can attribute the different cooling cycles influence the hardness values to the effect of cooling rate on the M_s point (the temperature at which martensite begins to form from austenite upon cooling) of the beads. Generally, martensite starting point M_s increases as cooling rate get enhanced. This is because the carbon distribution within the austenitic structure before transforming to the martensite was uneven. That is to say, most of the carbon atoms are segregated at the micro defect area such as vacancies and dislocations, and there will be forming "carbon clusters".

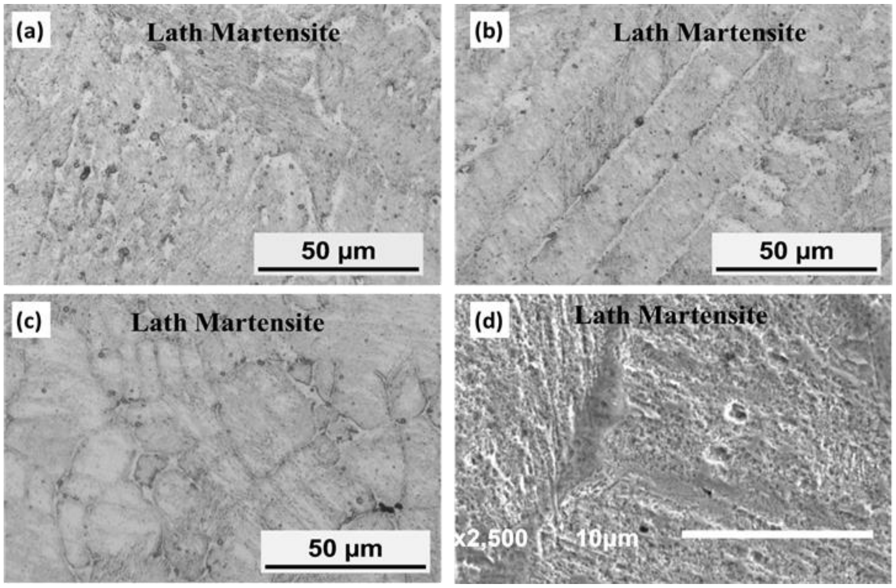

Figure 5: (a), (b) and (c) are the Optical Microstructures of Hybrid Laser-Arc Weld Beads After Cycle A, Cycle B and Cycle C Respectively, and (d) SEM Microstructure of Weld Bead After Cycle A

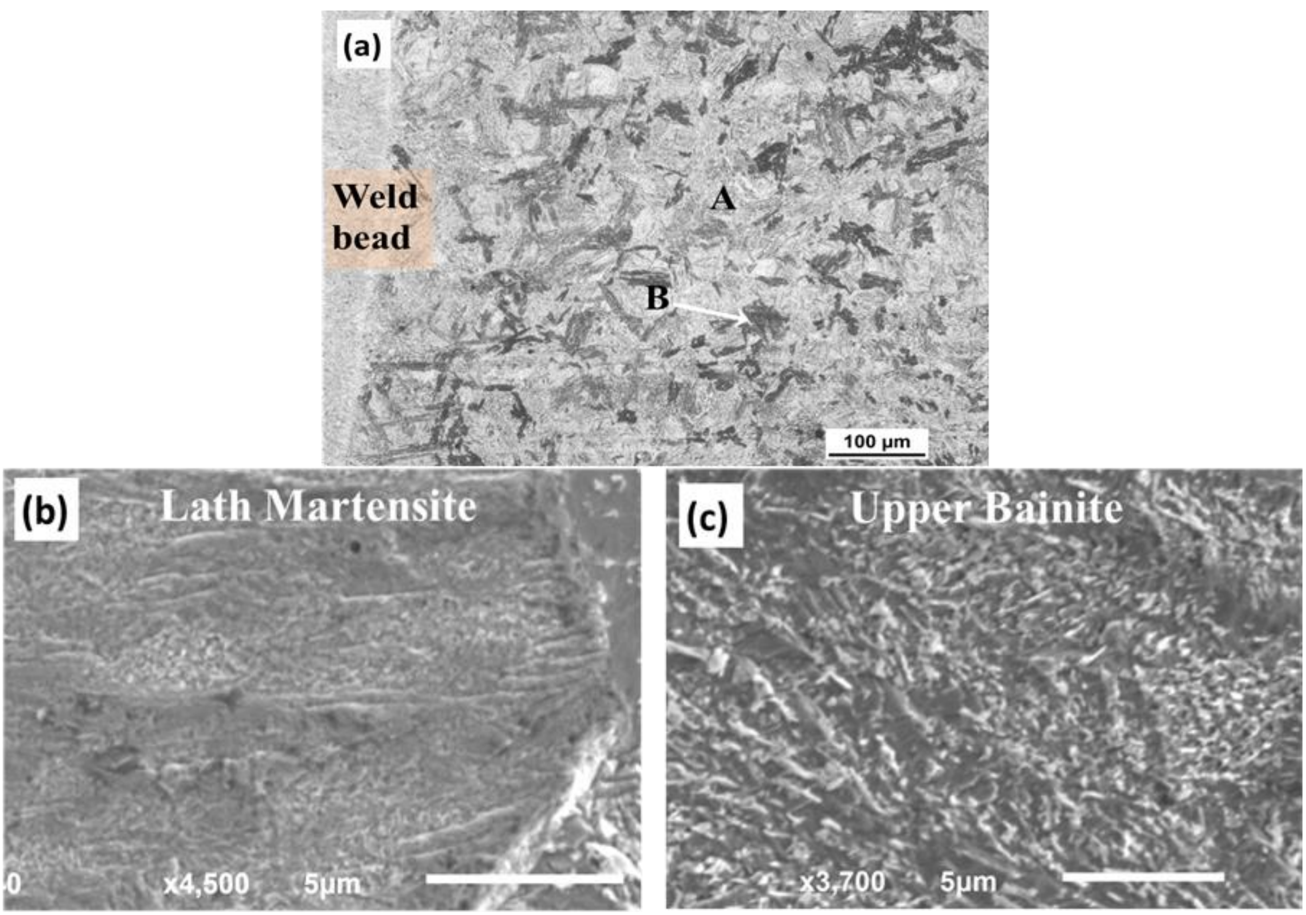

Figure 6: (a) Optical Microstructure of the Haz Near the Welded Bead for the Cycle B; (b) and (c) SEM of Microstructures at Points of Cycle A and B In (a).

The size of these "carbon clusters" depends mainly on the temperature. In other words, the carbon clusters are relatively large since the temperature was low. This is because at the low temperature, the activity of carbon atoms is weak, the atoms of carbon are easy to be segregated at the location of the dislocation, so it would be easy to form the "carbon clusters" and vice versa. So, when the cooling rate was small or cooling process was stopped at the austenitic region just like Cycle B and Cycle C, these "carbon clusters" can grow bigger enough. As a result, it can cling to the dislocations and obstruct the dislocation's movement. From the macro perspective, the austenite will be strong and difficult to be transformed to the martensitic phase, and so the M_s point will be lowered. Thus, the M_s point for the normal cooling process (Cycle A) must be higher than that of the Cycle B and C. Therefore, the amount of the transformed martensite for the Cycle A will be higher compared with the Cycle B and C.

The x-ray diffraction patterns for the beads added that, the peaks (γ (111) and γ (200) shown in Figure 10) of the austenitic structure for the Cycle A were lower than the other two, meaning retained austenite for the Cycle A must be smaller than that of Cycle B and Cycle C. Consequently, the hardness of the bead for the Cycle A was higher than that of the other two cycles.

In addition, as the carbon atoms have high activity in austenite, during fast cooling, the carbon clusters would be formed at very short time interval. So, the carbon clusters must be formed at the early stage for either the Cycle B (held at 400-500℃ for 400 sec) or the Cycle C (held at 400 - 500℃ for 900 sec). As a result, there would not be much of hardness difference between two cycles. That is to say, the hardness of the beads for the Cycle B and Cycle C are almost the same.

The hardness profiles within the HAZ varies with cooling process; the hardness values for the cycles A, B and C were HV450 -510, HV370 - 425, and HV320 - 375, respectively. This indicates that, the normal cooling process (Cycle A) has the highest hardness profile, secondly the thermal process of the 400sec-soaking process at 400 - 500℃ (Cycle B), thirdly the one which undergoes the 900sec-soaking process at 400-500℃ (Cycle C). In addition, under the three thermal cycles, as the middle of the HAZ reaches the highest hardness point, their peak values are 510, 425 and 375HV, respectively. Moreover, there is a narrow band beyond the HAZ with hardness as low as 330HV. These hardness trough bands are in fact the "softened bands", which commonly appear in high strength steels while they undergo welding process. Outside of the "softened bands" are the parent metal, and its harness remains at HV370 - 380.

The reason why the hardness values within the HAZ for the cycles A, B and C are orderly reduced was because when the HAZ undergoes the normal cooling process (Cycle A), the cooling curve bypasses the pearlite and/or bainite CCC-curve as the cooling speed was fast enough. So, the pre-austenite at the HAZ was totally transformed to the martensite. But for the Cycle B and Cycle C, which waited at the 400 - 500℃ for 400 sec and 900 sec while the temperatures drop, the cooling curves go through the upper bainite transformation zone of CCC-curve as shown in Figure 11. As a result, the upper bainite microstructures were formed within the HAZ for cycles B and C; because the longer the soaking time, the larger the amount of the upper bainite formed, so the amount of upper bainitic microstructures for the cycles B and C were relatively 38% and 62%. As already known, the hardness of the bainite is normally lower than that of the martensite. Therefore, it was revealed that the hardness values for cycles A, B and C decrease orderly.

Furthermore, the hardness peak which occurred in each cycle At the middle of the HAZ (Figure 9) can be explained as follows. For the HAZ nearer to the weld fusion line, there was a growth in lath size, so hardness will decrease gradually as we move from middle of HAZ towards the fusion line. Besides, progressing towards the parent metal from middle of HAZ, there was an increase in percentage of the low hardness pre-ferrite that was formed as the temperature reaches the Ac_1 and Ac_3 in the $Fe\text{-}Fe_3C$ diagram. In addition, this region also overlaps with the over-tempered zone. Therefore, hardness declines gradually as we progress from the peak hardness area to the outer part of the HAZ. Consequently, as the middle point of the HAZ forms 100 percent extremely fine and fresh lath-type martensite, the hardness value reaches the highest point of HV510.

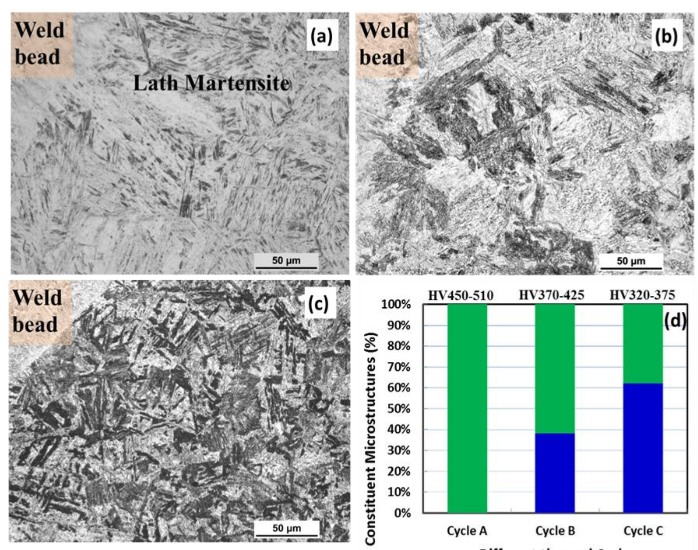

Figure 7: The Optical Microstructures of HAZ near the Welded Bead for the Cycles A (a), B (b), and C (c) Respectively, and (d) Percentage of the Constituent Microstructures.

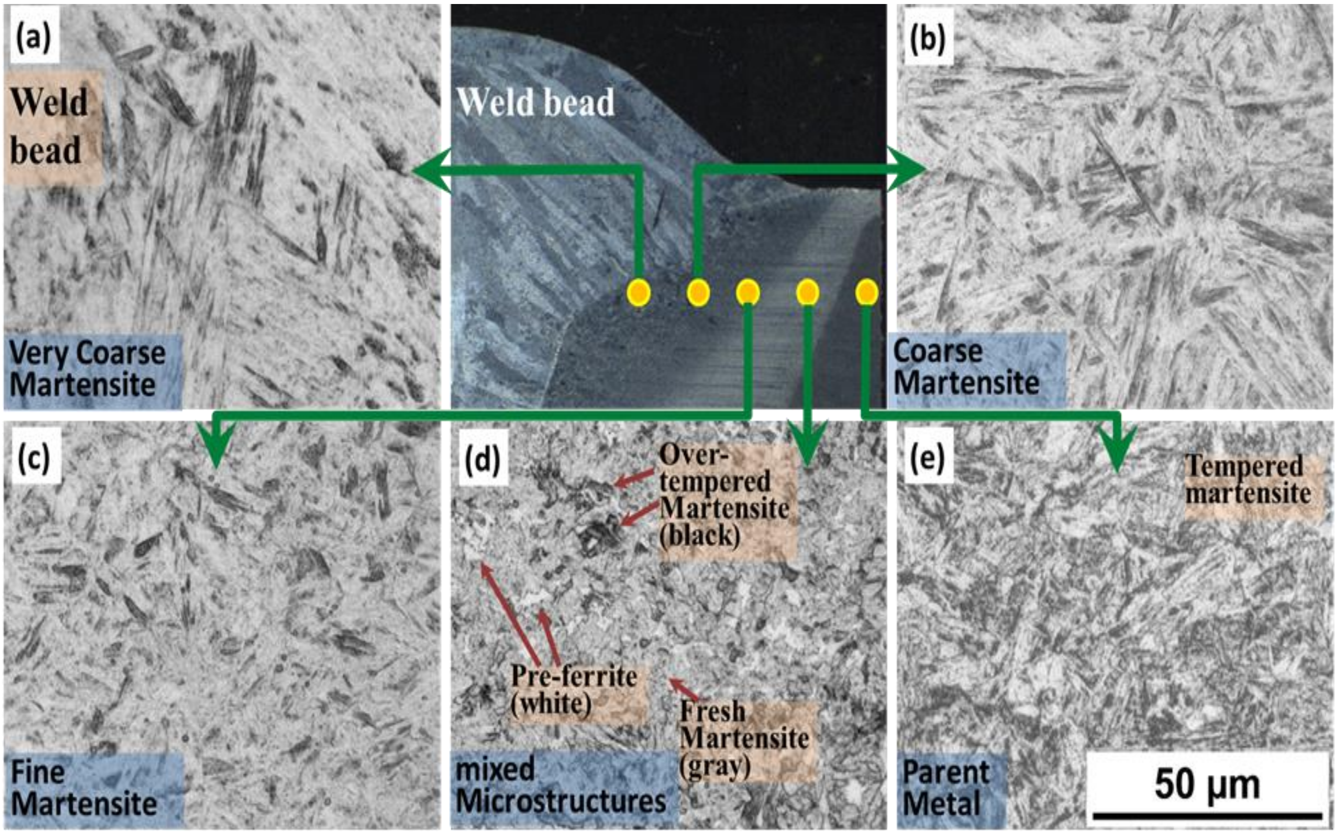

Figure 8: Optical Microstructures of the Haz for the Cycle A, (A)-(C) Revealing the Lath-Type Martensite in the Sequence from Coarse to Fine, (D) the Mixed Microstructures, and (E) the Parent Metal, Respectively

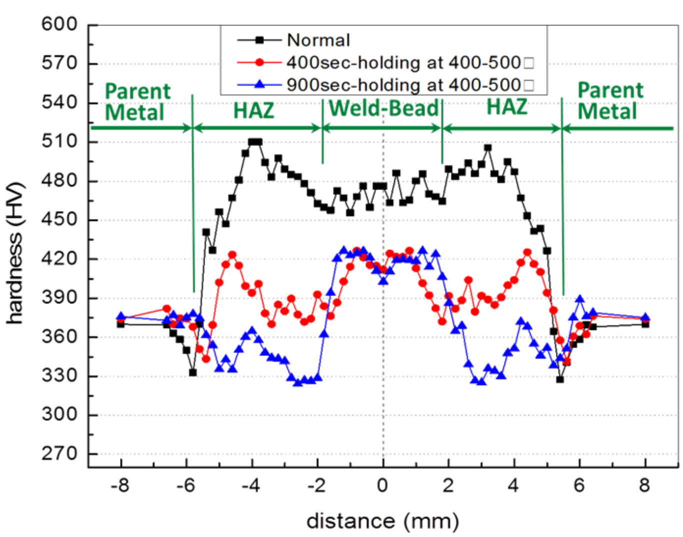

Figure 9: Hardness Profiles all Through the Whole Welded Joint at Cycles A, B and C

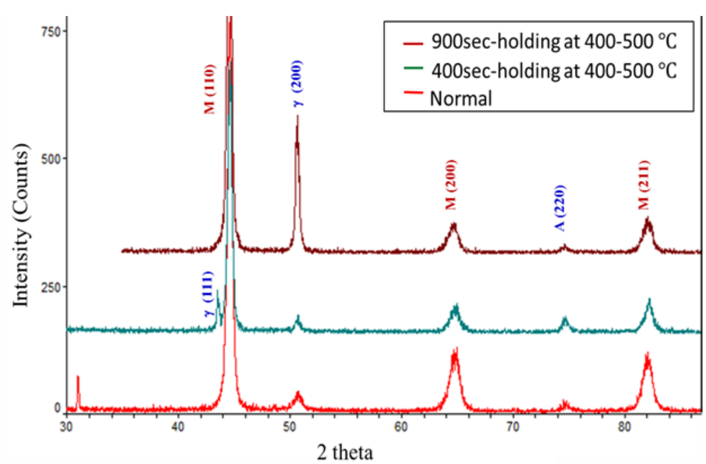

Figure 10: X-Ray Diffraction Patterns of the Weld Beads for the Cycle A (Red Line), Cycle B (Dark Blue Line), and Cycle C (Brown Line) Respectively.

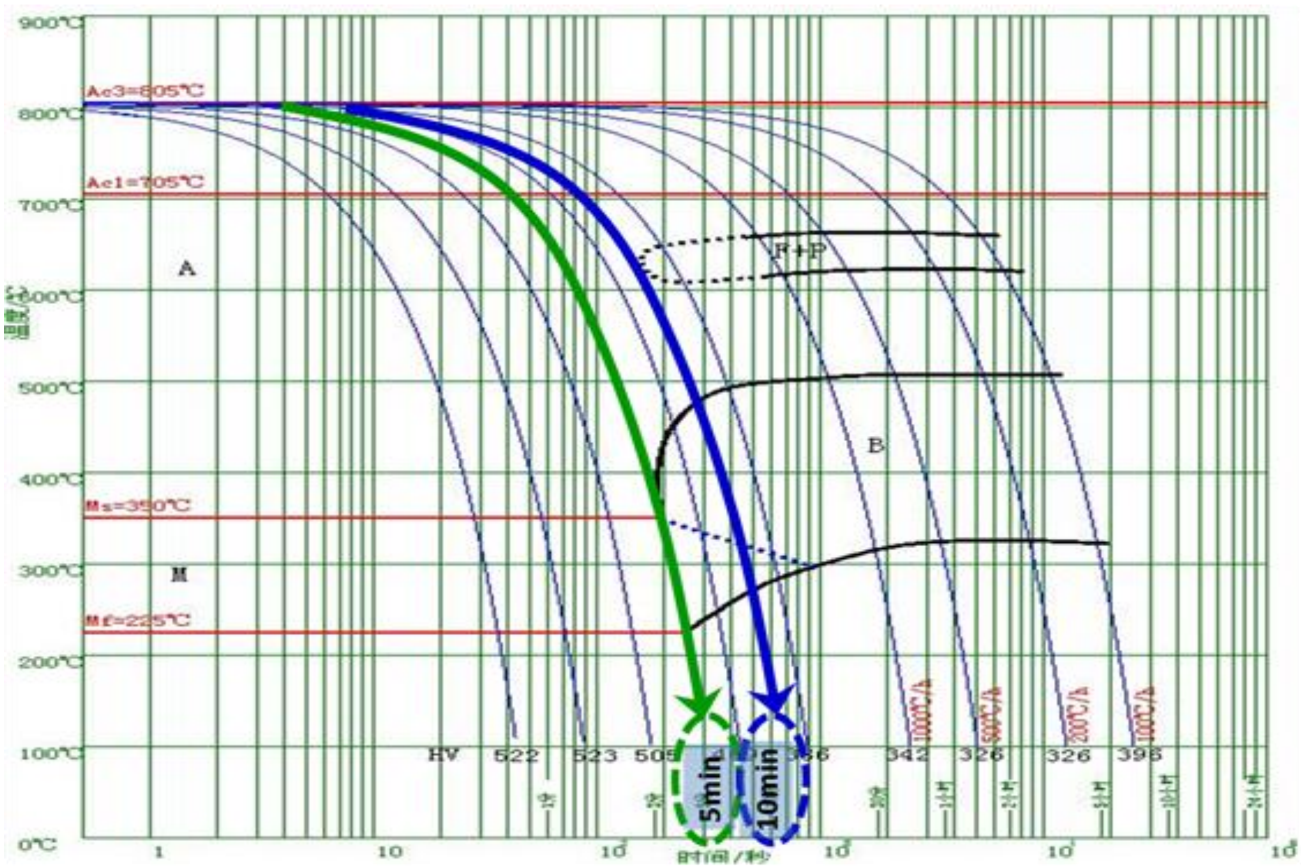

Figure 11: CCC Diagram for the High Strength Steel of 0.31c-0.34Si-0.85 mn-0.94cr-1.21Ni (Wt.%)

CONCLUSION

In this study, we have investigated hybid laser-arc welded joints of ultrahigh strength steel and it was found that the microstructures of all the weld beads consisted of lath martensitic structure with small percentage of retained austenite when cooling process undergoes the normal (Cycle A), 400 sec-soaking at 400 - 500℃ (Cycle B), and 900 sec-soaking at 400 - 500℃ (Cycle C), respectively. The microstructures formed at HAZ for cycles A, B and C consisted 0%, 38% and 62% of upper bainite respectively, while 100% martensite was formed during Cycle A.

As the low hardness upper bainite percentage of each cycle gradually increased, the hardness fluctuation ranged within the HAZ between 450 - 510, 370 - 425 and 320 - 375 respectively for Cycle A, B and C]. The hardness fluctuation values within the HAZ for the Cycle A, B and C are orderly 450 - 510, 370 - 425, and 320 – 375 HV, as the low hardness upper bainite percentage of the cycle gradually increased.

The middle of the HAZ reached the highest hardness point with peak values 510, 425 and 375 HV for the cycles A, B and C respectively. Outside of the HAZ, there was a narrow band, for which the hardness attained the lowest point of 330 HV. These hardness trough bands were the “soft bands”, which commonly appeared in the welding of high strength steels.

ACKNOWLEDGMENT

The opportunities accorded by the Chinese government and the Petroleum Technology Development Funds (PTDF) of Nigeria in providing necessary facilities and financial aid are invaluable, and the authors are grateful.

REFERENCES

Barényi, I., Híreš, O., and Lipták, P. (2013). Changes in Mechanical Properties of Armoured UHSLA Steel ARMOX 500 after Over Tempering. Problems of Mechatronics Armament, Aviation, Safety Engineering, 4(14), 7–14. https://doi.org/ISSN 2081-5891

Bunaziv, I., Frostevarg, J., Ren, X., Kaplan, A. F. H., and Akselsen, O. M. (2019). Porosity and solidification cracking in welded 45 mm thick steel by fiber laser-MAG process. Procedia Manufacturing, 36, 101–111. https://doi.org/ 10.1016 /j.promfg.2019.08.015

Cao, X., Wanjara, P., Huang, J., Munro, C., and Nolting, A. (2011). Hybrid fiber laser - Arc welding of thick section high strength low alloy steel. Materials and Design, 32(6), 3399–3413. https://doi.org/10.1016/j.matdes.2011.02.002

Chen, H., Guo, N., Zhang, X., Cheng, Q., Zhou, L., and Wang, G. (2020). Effect of water flow on the microstructure, mechanical performance, and cracking susceptibility of underwater wet welded Q235 and E40 steel. Journal of Materials Processing Technology, 277(2), 116435. https://doi.org/10.1016/j.jmatprotec.2019.116435

Frostevarg, J., and Kaplan, A. F. H. (2014). Undercuts in laser arc hybrid welding. Physics Procedia, 56(C), 663–672. https://doi.org/10.1016/j.phpro.2014.08.071

Kim, C. H., Ahn, Y. N., and Kim, J. H. (2011). CO2 laser-micro plasma arc hybrid welding for galvanized steel sheets. Transactions of Nonferrous Metals Society of China (English Edition), 21(SUPPL. 1), s47–s53. https://doi.org/10.1016/S1003-6326(11)61059-5

Kong, F., and Kovacevic, R. (2010). 3D finite element modeling of the thermally induced residual stress in the hybrid laser/arc welding of lap joint. Journal of Materials Processing Technology, 210(6–7), 941–950. https://doi.org/10.1016/j.jmatprotec.2010.02.006

Liu, J., Chen, C., Feng, Q., Fang, X., Wang, H., Liu, F., Lu, J., and Raabe, D. (2017). Dislocation activities at the martensite phase transformation interface in metastable austenitic stainless steel: An in-situ TEM study. Materials Science and Engineering A, 703, 236–243. https://doi.org/10.1016/j.msea.06.107

Ma, Z. H., Chen, D. G., Liu, H. W., and Yang, W. L. (2014). Microstructure and mechanical properties of welding joints of high nitrogen steel by hybrid laser-Arc welding. Applied Mechanics and Materials, 496–500, 444–447. https://doi.org/10.4028/www.scientific.net/AMM.496-500.444

Mazar Atabaki, M., Yazdian, N., and Kovacevic, R. (2018). Hybrid laser/arc welding of thick high-strength steel in different configurations. Advances in Manufacturing, 6(2), 176–188. https://doi.org/10.1007/s40436-017-0193-6

Ming, G., Xiaoyan, Z., and Qianwu, H. (2007). Effects of gas shielding parameters on weld penetration of CO2 laser-TIG hybrid welding. Journal of Materials Processing Technology, 184(1–3), 177–183. https://doi.org/10.1016/j.jmatprotec.2006 .11.019.

Němeček, S., Mužík, T., and Míšek, M. (2012). Differences between Laser and Arc Welding of HSS Steels. Physics Procedia, 39, 67–74. https://doi.org/10.1016/j.phpro.2012.10.015

Seede, R., Shoukr, D., Zhang, B., Whitt, A., Gibbons, S., Flater, P., Elwany, A., Arroyave, R., and Karaman, I. (2020). An ultra-high strength martensitic steel fabricated using selective laser melting additive manufacturing: Densification, microstructure, and mechanical properties. Acta Materialia, 186, 199–214. https://doi.org/10.1016/j.actamat.2019.12.037

Steen, W. (2004). Laser arc hybrid welding. In LIA Today (2nd Ed., Vol. 12, Issue 5). Elsevier Ltd. https://doi.org/10.1016/b978-0-08-101252-9.00009-1